International Journal of Engineering

Journal Homepage: www.ije.ir

Dynamic Response Analysis of a High Glide Ratio Parachute System

M. A. Ghapanvary*, M. Nosratollahi, J. Karimi

Department of Aerospace Engineering ,Malek-Ashtar University of Technology, Tehran, Iran

P A P E R I N F O

Paper history:
Received 19 September 2019
Received in revised form 10 September 2020
Accepted 14 October 2020

Keywords:
Multi-body System
Dynamic Response
Anhedral Angle
Gliding Path

A B S T R A C T

This paper is concerned with the dynamic stability study of a gliding parachute-payload system along its gliding path. To scrutinize the respective dynamic response characteristics after releasing from high altitude, a modified multi-body model is developed. In the stability analysis procedure, the yawing motion of the payload is considered in system dynamics, which in turn creates a state-dependent matrix in the stability analysis and makes the linearization algorithm more cumbersome. To solve the problem, a unified Jacobian-based symbolic differentiation algorithm is implemented and the dynamics is linearized about various operating points along gliding segment of a typical planned trajectory. Based on results, the system has short period and phugoid modes in longitudinal channel just like an aircraft. In addition to dutch roll mode, the system has a low frequency coupled roll-spiral mode in lateral-directional channel which is a result of effective canopy anhedral angle. It is shown, the coupled mode can be decomposed into two distinct roll and spiral modes for small anhedral angles. Based on results, as the parachute descends, both the period and damping ratio for the short period mode were increased by 18 and 30%, respectively. For the phugoid mode the period of oscillations is decreased by 20% and the damping ratio, almost remains constant. For the lateral-directional channel,. As the parachute descends, the dutch roll mode is destabilized whereas the other modes are stabilized. Furthermore, from a practical point of view, lengthening the suspension lines stabilizes the coupled roll-spiral mode whereas destabilizes the other modes.

***doi**: 10.5829/ije.2021.34.01a.22*

NOMENCLATURE

S_C	Canopy reference area (m^2)	**Greek Symbols**	
$[f_O]^G, [m_O]^G$	Constraint force and mpment vector acting on the confluence point (N, N.m)	ϕ_G, θ_G, ψ_G	Paylod Euler angles (deg)
I_G^G, I_P^P	Mass moment of inertia tensors for the gliding parachute and payload ($kg.m^2$)	μ	Canopy Rigging Angle (deg)
m^{G+A}, m^P	Mass of parachute and included air mass, mass of the payload (kg)	**Subscripts**	
s_{PO}, S_{PO}	Canopy reference area (m^2)	C, G, E, P	Canopy, gliding parachute, earth, payload frames

1. INTRODUCTION

Basically, a high glide ratio cargo delivery parachute is deployed from high altitude to attain a large stand-off distance and so may experience different trim conditions through the gliding segment of their trajectory. Parachute system can be perturbed from its trim condition, in presence of a disturbance. In this situation, when the parachute system returns to its initial trim point, it is called an asymptotically stable system. As, it achieves a new trim condition; it is called a marginally or neutrally stable and otherwise it is called an unstable system. Up to now, several researches were carried out about the dynamics and stability analysis of different systems such as torsional micro-actuators [1], axis gimbal system [2]. Also, many studies are devoted to investigate the control of the system vibration and oscillatory platforms. In this respect, the stability of the

*Corresponding Author Institutional Email: *ma.ghapanvary@isrc.ac.ir* (M. A. Ghapanvary)

Please cite this article as: M. A. Ghapanvary, M. Nosratollahi, J. Karimi, Dynamic Response Analysis of a High Glide Ratio Parachute System, International Journal of Engineering, Transactions A: Basics Vol. 34, No. 01, (2021) 195-201

system was provided with a fuzzy controller [3]. Oscillatory transporting Platform was used to sieving extremely wet earth mass [4]. The vibration of a system was controlled using tuned mass dampers [5]. Meanwhile, due to the highly coupled dynamics and complex behavior of the parachute and payload system, its stability has not been extensively discussed, as yet. However, in some studies, the stability analysis of the system was evaluated for a simplified model at sea level. The parachute stability characteristics were considered as a function of the inertia properties of the payload and obtained that the damping ratio and period were increased as related inertia increased [6]. The center of gravity and lift coefficient limits for a parachute were analyzed and various conditions and expressions for forward and backward center of gravity limits were given in literature [7]. The effects of scale and wing loading on a parachute using a linearized model for aerodynamic coefficients were studied in literature [8]. The lateral mode of parachute with a simplified model for a personnel-type parachute was modeled but the effect of apparent mass and inertia were not considered in the analysis [9].

The apparent mass force and moment coefficients were proposed by Lissaman and Brown [10]. Also, it was reported that canopies with wing loading less than 5kg/m^2 suffered from adverse effects of apparent mass during motion. It has been reported by Lingard [11], that by increasing the line length may destabilize the parachute whereas increasing the altitude had a stabilizing effect for the parachute. Also was concluded that increasing the aspect ratio resulted in increasing the static stability. The stable trim points were extracted using bifurcation analysis [12]. The main disadvantage of this method is stringent dependency of analysis to initial conditions. Moreover, several researches have been performed to model the behavior and dynamic response of the parachute systems. These works are summarized to model the parachute dynamics with different degrees of freedom and to study the system dynamics behavior. Usually, low-fidelity models with a reduced order were used to design the guidance, navigation and control (GNC) system. In this respect, a model with 4-DOF was presented which consist of planar dynamics with capability to roll and yaw [13]. Some models with 6-DOF were introduced in literature [14,15] that considered the parachute and payload system as a single rigid body system. Another 6-DOF model was presented in which the longitudinal mode was controlled by changing canopy incidence [16]. Turn response to asymmetric deflections and response to the gust was simulated using an 8-DOF model [17]. Another 8-DOF model was developed by Redelinghuys [18] for parachute with a suspended Unmanned Aerial Vehicle (UAV) and so the additional analytical constraints were added to the equations of motion. Other 8-DOF model with payload pitching and yawing motion was presented in which the constraint forces and moments were analytically solved during solving equations of motion. A comparison between 7-DOF and 8-DOF models was carried out and it is shown that a 7-DOF can describe the parachute dynamics when payload was connected in four points. Therefore, in case of a four-point connection of parachute to the payload, the payload yawing motion can disturb the overall system's response. Specially, when speaking about the lateral-directional responses, separation of the parachute and payload into one connection point leads to rolling, pitching and yawing motion with respect to the canopy which needs to a 9-DOF model. In this respect, different 9-DOF models were developed. It was assumed that there was only asymmetric TE deflection which was used to control the parachute in lateral-directional channel and the longitudinal channel was controlled by varying the canopy incidence angle [19]. Therefore, the symmetric brake deflection is replaced with canopy incidence angle in equations of motion. Mooij et al. [20] presented method similar to the approach proposed by Slegers and Castello [21], the equations of motion were solved simultaneously with constraint forces and moments, whereas in analytical dynamics required artificial constraint stabilization to satisfy the constraint at the confluence point [22]. The parachute systems had two modes of short period and phugoid in longitudinal channels and roll, duch roll and spiral modes in lateral-directional channel. In recent studies, using a 6-DOF linearized model discussed in litrature [23, 24], a dynamic stability study was carried out for a powered low anhedral canopy parachute. The eigenvalues of longitudinal and lateral-directional channels were obtained whereas the trim points were extracted through a static 4-DOF model of straight trimmed flight in which the effect of relative pitching motion of the payload on the dynamic modes was considered.

Clearly, achieving a large gliding distance necessitates releasing the gliding platform from a high altitude which in turn results in a wide variation of air density. This changes the parachute velocity from release to the impact points. Moreover, the apparent mass and inertia terms and so the dynamic response will change due to this variation. Evidently, in order to design of a gliding parachute, it is necessary to take the stability characteristics into account. Therefore, since the flight condition is varying, it is important to investigate the trend of the dynamic stability over the flight envelope.

On the other hand, as a significant design variable for gliding parachutes, the anhedral angle can affect the dynamic response as well as the gliding capability. The effective values of this design variable may result in different lateral-directional dynamics. Therefore, this paper is inspired by these problems to study each mode of system dynamics at different operating points along the gliding flight path. In other wods, the effect of

variation of altitude and the anhedral angle, which is the most important control parameter in lateral channel, on each dynamic mode of the system is scrutinized. This issue was ambiguously discussed in aforementioned studies. Herein, the yawing motion of the payload is considered in system dynamics creates a state-dependent matrix in dynamic equations which has not been considered for the parachute-payload system as yet. So, due to the complexity of the linearization of the airdrop system, the stability analysis procedure is difficult and time-consuming. This paper presents a unified jacobian-based symbolic differentiation algorithm that the system of equations is linearized by means of the algorithm.

2. PARACHUTE MODEL DESCRIPTION

For a parachute system model, when parachute and payload are considered as separate bodies, components of constraint forces and moments will be appeared. Hence, the rotational motion of the payload in space can be expressed as a combination of parachute rotational motion in space and a relative yawing motion. So, to avoid prolonging the paper with repetitive relationships, a model is used and modified for longitudinal trailing edge control surface instead of incidence angle, as longitudinal control input.

The schematic of the high glide ratio parachute-payload system is shown in Figure 1. Based on the figure, there are 4 different reference frames for deriving equations of motion. These frames are attached to the canopy, gliding parachute (includes the canopy and suspension lines), payload and earth as an inertial reference frame.

By rearranging the translational, rotational and kinematic constraint equations, the complete set of equations of motion which describes the parachute-payload dynamics is summarized in a nonlinear state-space form as below:

$$M\dot{X} = F \tag{1}$$

In which the respective matrices are as follows :

$$\begin{bmatrix} m^{G+A}+[J_M]^G & -m^{G+A}[S_{GO}]^G+[J_M]^G & 0_{3\times3} & 0_{3\times1} & 0_{3\times1} & -I_{3\times3} & 0_{3\times2} \\ m^P[T]^{PG} & -m^P[S_{PO}]^P[T]^{PG} & 0_{3\times3} & -[S_{PO}]^P & 0_{3\times1} & [T]^{PG} & 0_{3\times2} \\ [S_{MG}]^G[J_M]^G & [I_G^G]^G+[J_M]^G-[S_{MG}]^G[J_M]^G & 0_{3\times3} & 0_{3\times1} & 0_{3\times1} & -[S_{OG}]^G & 0 \\ 0_{3\times3} & [I_P^P]^P & 0_{3\times3} & [I_P^P]^P & 0_{3\times1} & [S_{GP}]^P & [T]^{PG} \\ 0_{3\times3} & 0_{3\times3} & I_{3\times3} & 0_{3\times1} & 0_{3\times1} & 0_{3\times3} & 0_{3\times2} \\ 0_{1\times3} & 0_{1\times3} & 0_{1\times3} & 0 & 1 & 0_{1\times3} & 0_{1\times2} \end{bmatrix} \begin{bmatrix} \dot{V}_O^E \\ \dot{\omega}^{GE} \\ \dot{\phi}_G \\ \dot{\theta}_G \\ \dot{\psi}_G \\ \dot{r}_P \\ \dot{\psi}_P \\ F_O \\ M_{Ox} \\ M_{Oy} \end{bmatrix} = \begin{bmatrix} F_1 \\ F_2 \\ F_3 \\ F_4 \\ F_5 \\ F_6 \end{bmatrix} \tag{2}$$

in which the right hand side expression for the force and moments can be expressed as:

$$\begin{aligned}
F_1 &= -m^{GA}[\Omega^{GE}]^G[V_O^E]^G - m^{GA}[\Omega^{GE}]^G[\Omega^{GE}]^G[s_{GO}]^G - [\Omega^{GE}]^G[J_M]^G[V_O^E]^G + \dots \\
&\quad [\Omega^{GE}]^G[J_M]^G[S_{MO}]^G[\omega^{GE}]^G - [\Omega^{GE}]^G[J_M]^G[T]^{GL}[V_A^E]^L + m^G[T]^{GL}[0\ 0\ g]^T + [f_{aero_G}]^G \\
F_2 &= -m^P[T]^{PG}[\Omega^{GE}]^G[V_O^E]^G - m^P[\Omega^{GE}]^G[\Omega^{GE}]^G[S_{Po}]^P + m^P[S_{Po}]^P[\Omega^{PG}]^P[T]^{PG}[\omega^{GE}]^G + \dots \\
&\quad m^P[T]^{PG}[T]^{GL}[0\ 0\ g]^T + [f_{aero_P}]^P \\
F_3 &= -[\Omega^{GE}]^G[I_G{}^G]^G[\omega^{GE}]^G - [\Omega^{GE}]^G[J_M]^G[\omega^{GE}]^G - [S_{MG}]^G[\Omega^{GE}]^G[J_M]^G[V_O^E]^G + \dots \\
&\quad [S_{MG}]^G[\Omega^{GE}]^G[J_M]^G[S_{MO}]^G[\omega^{GE}]^G + [S_{MG}]^G[\Omega^{GE}]^G[J_M]^G[T]^{GL}[V_A^E]^L + \dots \\
&\quad [S_{GC}]^G[f_{aero_G}]^G + [m_{aero_{C/4}}]^G + [0\ 0\ m_{OZ}{}^P]^T + [S_{LG}]^G[f_{aero_{Lines}}]^G \\
F_4 &= -[\Omega^{PE}]^P[I_P{}^P]^P[\omega^{PE}]^P - [T]^{PG}[0\ 0\ m_{OZ}{}^P]^T + [I_P{}^P]^P[\Omega^{PG}]^P[T]^{PG}[\omega^{GE}]^G \\
F_5 &= [1\ \sin\phi_G\tan\theta_G\ \cos\phi_G\tan\theta_G \mid 0\ \cos\phi_G\ -\sin\phi_G \mid 0\ \sin\phi_G/\cos\theta_G\ \cos\phi_G/\cos\theta_G][\omega^{GE}]^G \\
F_6 &= r_P - r_G
\end{aligned} \tag{3}$$

Using lyapunov indirect method herein, local response characteristics are obtained for the decoupled dynamics with varying trim points. Since the state matrix is state dependent, the conventional differentiation is not applicable. For this purpose, the state matrix is inverted and taken to the right hand side of the equation. Then the Jacobian operator is applied to linearize the unified symbolic expression. Finally, by expressing the equations of motion in a compact form (2), the nonlinear system can be written in a matrix form as below:

$$\begin{aligned}
&M\dot{x} = f(\bar{x},\bar{u}) \\
&\bar{x} = [u_o, v_o, w_o, p_G, q_G, r_G, \phi_G, \theta_G, \psi_G, r_P, \psi_P] \\
&\bar{u} = [\delta s, \delta u]
\end{aligned} \tag{4}$$

Herein, the system dynamics should be linearized about an operating point including system states and control inputs. The inputs of the system dynamics are symmetric and asymmetric trailing edge deflections during a steady gliding flight. Therefore, equilibrium points vector can be assigned as follows:

$$\bar{X}_{eq} = [u_0, 0, w_0, 0, 0, 0, 0, \theta_0, 0, 0, 0], \ \bar{U}_{eq} = [0, 0] \tag{5}$$

Based on lyapunov linearization method, a nonlinear system has a behavior similar to its linear model in small motion intervals [20]. In order to study the effect of each input on system response, it is necessary to omit the other inputs, thus the control inputs are set to be zero. So, the parachute system which has relatively slow dynamics, can be linearized about its operating points as an invariant system as follows:

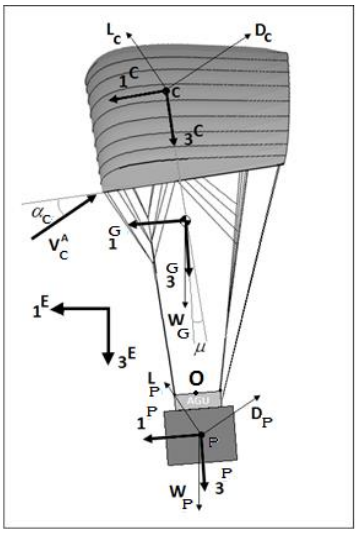

Figure 1. High glide ratio parachute-payload system

$$\Delta\dot{x} = A\Delta x + B\Delta u$$
$$A = \frac{\partial(M^{-1}f)}{\partial x}_{(x=x_0,u=u_0)} \quad (6)$$
$$B = \frac{\partial(M^{-1}f)}{\partial x}_{(x=x_0,u=u_0)}$$

It should be noted that, since the matrix M is state dependent and a function of the payload relative yawing angle, the inverse of matrix M should be considered in calculating the Jacobian matrix in linearization procedure. In this respect, the diagram of the dynamic stability analysis procedure of parachute-payload assembly is shown in Figure 2.

As shown in Table 1, to compare the present algorithm with a practical case, the methodology is used to determinte ALEX PADS modes. As a desireable matching and ignorable errors, the algorithm is verified and consequently is applicable for all parachute models.

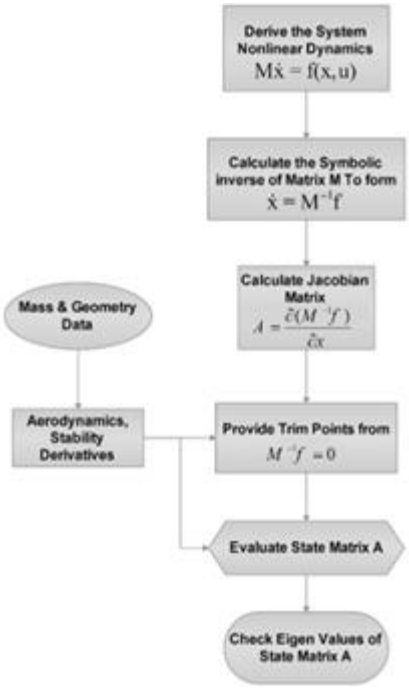

Figure 2. Novel algorithm flowchart for dynamic stability analysis of multi-body parachute-payload system

TABLE 1. Estimation of Alex dynamic modes [26]

Dynamic Mode	Period (s)	Estimated period (s)	Damping Ratio	Estimated Damping Ratio
Short period	1.1	1.2	0.58	0.5
Phugoid	8.4	8.3	0.4	0.36
Dutch Roll	1.8	1.87	0.19	0.2
Roll-Spiral	6.7	7.06	0.47	0.5

Now, a high penetrating GPDAS platform with a maximum 1000 kg rigged cargo, the dynamic response can be studied. The platform can achieve a desired stand-off distance of more than 30km. The parachute specifications are listed in Table 2.

3. RESULTS AND DISCUSSION

In order to investigate the dynamic behavior of the present parachute, two cases were considered in which several trim points are obtained for different altitudes along the gliding path, for a fix payload mass and different anhedral angles. The extracted trim points along the gliding path are given in Table 3. As can be seen in the table, from the maximum operational altitude to minimum level, the velocity decreases gradually whereas the pitch angle remains constant for a fix rigging scheme.

The root loci for the longitudinal channel modes are illustrated in Figure 3. The arrows show the direction of increasing in altitude from the sea level to its maximum value. Based on results, as the parachute descends, both the period and damping ratio for the short period mode are increased by 18 and 30%, respectively. For the phugoid mode the period of oscillations is decreased by more than 20% whereas it's damping ratio, almost remains constant. Overally, the systems stability level in longitudinal channel is improved during the parachute descend. In other words, applying brakes at high altitudes to control the glide ratio may deteriorate the system longitudinal stability particularly in faster mode.

TABLE 2. Parachute specification

Parameter	Value
Chord (m)	5.5
Span (m)	16.5
Rigging angle (deg)	2
Parachute mass (kg)	32
Number of main Lines	40
Line diameter (mm)	0.003
Line Length to span ratio	0.85
Payload Dimensions (m)	1*1*1

TABLE 3. Trim points along the gliding path

h (m)	Uc (m/s)	Wc (m/s)
0	15.49	2.61
2500	17.54	2.95
5000	20	3.37
7500	23	3.87
9000	25.14	4.23

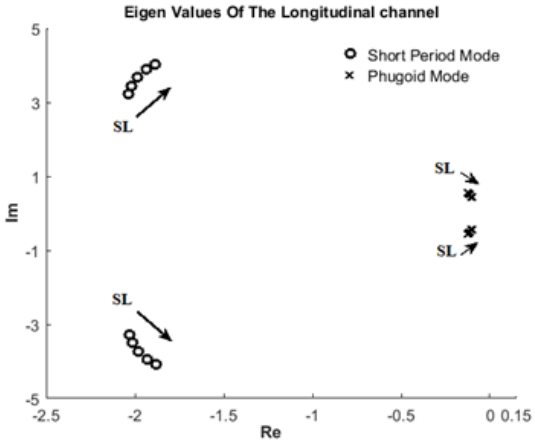

Figure 3. Root locus of the longitudinal modes

On the other hand, the root loci for the lateral-directional modes are provided as shown in Figure 4. Based on results, the lateral-directional modes include a pair of complex conjugate root which characterizes the dutch roll mode and another pair of complex conjugate root which introduces a coupled roll-spiral mode. The arrows show the direction of increasing in altitude from the minimum to its maximum value.

For arced circular canopies, increasing the anhedral angle will decrease the line length which leads to a small rolling moment. Hence, the resultant rolling and yawing moments produce a coupled roll-spiral mode in which roll and spiral modes are combined together. The vlaues of line length and trim points evaluated at lowest altitude, are given in Table 4.

Based on the above results, when the line length increases, the damping of the coupled roll spiral mode tends to 1 and so the combined mode decomposes into two real eigenvalues which represent the conventional roll and spiral modes. The root loci of the longitudinal and lateral-directional channels are shown in Figures 5 and 6, respectively. Based on results, in longitudinal channel, variation of the suspension line length has a significant effect on phugoid damping whereas the short period damping changes slightly.

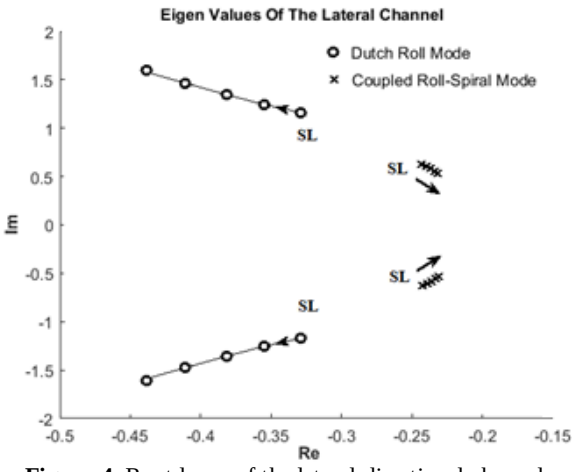

Figure 4. Root locus of the lateral-directional channel

TABLE 4. Anhedral angles and respective trim points

Anhedral Angle (deg)	$\frac{R_{Lines}}{b}$	Uc (m/s)	Wc (m/s)	θ(deg)
32.70	0.6	15.5	3.18	-4.30
15.0	1	15.36	2.54	-4.13
9.74	1.5	14.99	2.49	-3.89
7.24	2	14.76	2.51	-3.82
5.76	2.5	14.58	2.54	-3.80

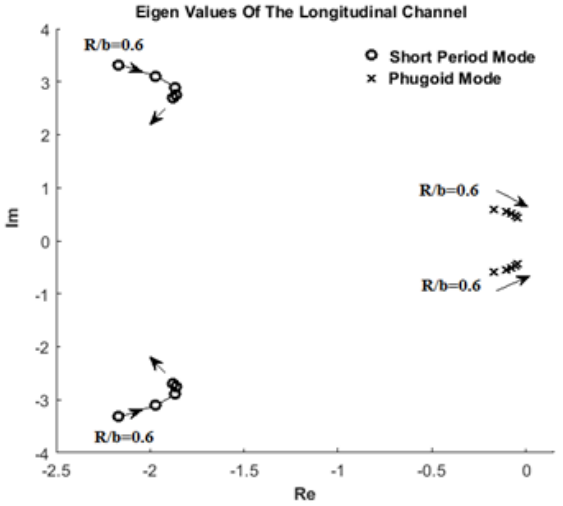

Figure 5. Root locus of the longitudinal modes for different anhedral angles

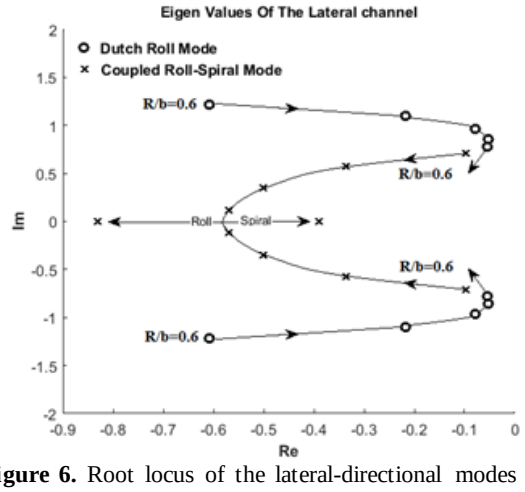

Figure 6. Root locus of the lateral-directional modes for different anhedral angles

Also, for the lateral-directional channel, both the dutch roll and coupled roll-spiral modes change considerably. In fact, the values of the line to span ratio from 1.5 to 2 are not practical but show how the root loci move in s-plane. In all channels the period of the dynamic modes is directly proportional to the suspension line length. In other words, the higher the line length is, the higher the period of all modes becomes. Hence, for the practical values of the line length, except the coupled roll-spiral mode in the lateral-directional channel, increasing the line length will decrease the levels of stability in the other modes, i.e. short period, phugoid and dutch roll.

4. CONCLUSION

In order to realize the gliding parachute dynamic behavior over the gliding envelope, using a multi-body model, the dynamic stability of a large gliding parachute-payload assembly was studied. The eigenvalues for different trim points along the gliding segment were obtained for decoupled longitudinal and lateral-directional channels.

Unlike the conventional flying vehicle modes, the roll and spiral modes of the present gliding parachute were coupled to each other that arose from effective anhedral angle of the canopy. The coupled roll-spiral mode has a higher damping ratio as compared to the lightly damped dutch roll mode. The dynamic stability analysis showed that, as the parachute glided from the maximum operational altitude to the sea level, the system stability level in longitudinal channel was improved. In this respect, the period and damping ratio of the short period mode were increased. For the phugoid mode, the period was decreased whereas its damping ratio almost remained constant. For the coupled roll-spiral mode, both the period and the damping ratio of oscillations were slightly decreased. As the parachute descended, among the dynamic modes, the dutch roll mode along the gliding path was destabilized. Therefore, as a worst case for evaluating the level of stability of the system modes particularly in conceptual design phase, it is recommended to perform the systems dynamic stability analysis at maximum operational altitude for the short period mode and at minimum altitude for the dutch roll mode. On the other hand, the eigenvalues were extracted for different line length to analyze the effect of the anhedral angle on system dynamics, especially in coupled mode. Based on results, in longitudinal channel, changing the suspension line length had a significant effect on phugoid damping whereas the short period damping was slightly changed. Also, for the lateral-directional channel, both the dutch roll and coupled roll-spiral modes were considerably changed. In all channels, the period of the dynamic modes was directly proportional to the suspension line length. So, the higher the line length was, the higher the period of all modes became. Based on results, as the parachute descends, both the period and damping ratio for the short period mode were increased by 18 and 30%, respectively. For the phugoid mode the period of oscillations was decreased by more than 20% whereas it's damping ratio, almost remained constant. Generally, the system stability level in longitudinal channel was improved during the parachute descend.

In all channels the period of the dynamic modes was directly proportional to the suspension line length. Hence, for the practical values, except the coupled roll-spiral mode of the lateral-directional channel, increasing the line length decreased the levels of stability for the other modes. In addition, increasing the line to span ratio by twice herein, resulted in separation of the roll and spiral modes from each other. So the suspension line length which represented the canopy anhedral angle, was the main responsible for the mentioned coupled roll-spiral mode. For the practical values of the suspension line length, only the coupled roll-spiral mode showed improving in the system stability with lengthening the lines whereas the other modes were destabilized. Also, the linearized symbolic model was verified by comparing the results with an available parachute data, with a negligible error in prediction of the dynamic modes. Therefore, the model could be used during design cycle and was applicable to all gliding parachutes

5. REFERENCES

1. Abbasnejad B., Shabani R., Rezazadeh G., Stability Analysis in Parametrically Excited Electrostatic Torsional Micro-actuators, International ***Journal of Engineering, Transactions C: Aspects***, Vol. 27, No. 3, (2014) 487-498. DOI: 10.5829/idosi.ije.2014.27.03c.17.
2. Pirzadeh M., Toloei A. R., Vali A. R., 'Effects of Flight Dynamics on Performance of One Axis Gimbal System, Considering Disturbance Torques', ***International Journal of Engineering, Transactions B: Applications***, Vol. 28, No. 8, (2015) 1108-1116. DOI : 10.5829/idosi.ije.2015.28.08b.01.
3. Berdnikov V., Lokhin V.,'Synthesis of Guaranteed Stability Regions of a Nonstationary Nonlinear System with a Fuzzy Controller', ***Civil Engineering Journal***, Vol. 5, No. 1, (2019), DOI: 10.28991/cej-2019-03091229.
4. Mihajlović G., Živković M.,' Sieving Extremely Wet Earth Mass by Means of Oscillatory Transporting Platform', ***Emerging Science Journal***, Vol. 4, No. 3 (2020) 172-182. DOI: 10.28991/esj-2020-01221
5. Rahimi F., Aghayari R., Samali B.,'Application of Tuned Mass Dampers for Structural Vibration Control: A State-of-the-art Review', ***Civil Engineering Journal***, Vol. 6, No. 8, (2020), 1622-1651. DOI: 10.28991/cej-2020-03091571
6. Hailiang M., Zizeng Q.,'9-DOF Simulation of Controllable Parachute System for Gliding and Stability', ***Journal of National University of Defense Technology***, Vol. 16, No. 2, (1994), 49–54.

7. Iosilevskii G (1995) Center of Gravity and Minimal Lift Coefficient Limits of a Gliding Parachute. ***Journal of Aircraft***, Vol. 32, No. 6, 1297-1302. DOI: 10.2514/3.46878
8. Brown, G. J., 'Parachute Steady Turn Response to Control Input', Aerospace Design Conference, Irvine, CA, USA, (1993). DOI: 10.2514/6.1993-1241
9. Crimi P (1990) Lateral Stability of Gliding Parachutes. ***Journal of Guidance, Control and Dynamics,*** Vol. 13, No. 6, 1060-1063. DOI: 10.2514/3.20579
10. Lissaman, P, Brown G, "Apparent Mass Effects on Parachute Dynamics. Aerospace Design Conference", Irvine, California, USA. (1993), DOI : 10.2514/6.1993-1236
11. Lingard J. S., 'Ram-air Parachute Design'.13th AIAA Aerodynamic Decelerator Systems Technology Conference; Clearwater Beach, Florida, USA, (1995).
12. Prakash O., Daftary A., Ananthkrishnan A., 'Bifurcation Analysis of Parachute-Payload System Flight Dynamics', AIAA Atmospheric Flight Mechanics Conference and Exhibit; San Francisco, California, USA, (2005). DOI: 10.2514/6.2005-5806
13. Jann, T Advanced Features for Autonomous Parachute Guidance, Navigation and Control. 18th AIAA Aerodynamic Decelerator Systems Technology Conference and Seminar; Munich, Germany, (2005). DOI: 10.2514/6.2005-1642
14. Barrows T Apparent Mass of Parachutes with Spanwise Camber. ***Journal of Aircraft***, Vol. 39, No. 3, (2002), 445-451. DOI: 10.2514/2.2949
15. Zhang Z, Zhao Z, Fu Y., 'Dynamics analysis and simulation of six-DOF parafoil system', ***Cluster Computing***, Vol. 22, No. 5, (2018), 1-12. DOI: 10.1007/s10586-018-1720-3
16. Slegers N., Beyer E., Costello M., 'Use of Variable Incidence Angle for Glide Slope Control of Autonomous Parachute'. ***Journal of Guidance, Control, and Dynamics***, Vol. 31, No. 3, (2008), 585-596. DOI: 10.2514/1.32099
17. Müller S, Wagner O, Sachs G. 'A High-Fidelity Nonlinear Multibody Simulation Model for Parachute Systems,, 17th AIAA Aerodynamic Decelerator Systems Technology Conference and Seminar; Monterey, California, (2003). DOI: 10.2514/6.2003-2120
18. Redelinghuys C.,'A Flight Simulation Algorithm for a Parachute Suspending an Air Vehicle', ***Journal of Guidance, Control, and Dynamics***, Vol. 30, No. 3, (2007), 791-803. DOI: 10.2514/1.25074
19. Slegers N Effects of Canopy-Payload Relative Motion on Control of Autonomous Parachute. ***Journal of Guidance, Control, and Dynamics***, Vol. 33, No. 1, (2010), 116-125. DOI: 10.2514/1.44564
20. Mooij E, Wijnands Q, Schat, B.,'9-DOF Parachute/Payload Simulator Development and Validation', AIAA Modeling and Simulation Technologies Conference and Exhibit; Austin, Texas, USA, (2003). DOI: 10.2514/6.2003-5459
21. Slegers N., Castello M.,' spects of Control for a Parachute and Payload System', ***Journal of Guidance, Control and Dynamics***, Vol. 26, No. 6, (2003), 898-905. DOI: 10.2514/2.6933
22. Strickert G., Jann T., 'Determination of the Relative Motion Between Parachute Canopy and Load Using Advanced Video-Image Processing Techniques', 15th Aerodynamic Decelerator Systems Technology Conference; Toulouse, France, (1999), DOI: 10.2514/6.1999-1754
23. Yang H., Song L., Chen W., 'Research on parachute stability using a rapid estimate model', ***Chinese Journal of Aeronautics***, Vol. 30, No. 5, (2017), 1670-1680. DOI: 10.1016/j.cja.2017.06.003
24. Gorman C. M., Slegers N. J., 'Comparison and Analysis of Multi-body Parafoil Models With Varying Degrees of Freedom', 21th AIAA Aerodynamic Decelerator Systems Technology Conference and Seminar, Dublin, Ireland, (2011). DOI: 10.2514/6.2003-5611
25. Slotine J J., Lee W., Applied nonlinear control. New Jersey: Prentice-Hall Inc, (1991).
26. O. A. Yakimenko, 'Precision Aerial Delivery Systems: Modeling, Dynamics, and Control. Progress in astronautics and aeronautics', American Institute of Aeronautics and Astronautics, Inc. Volume 248. Virginia:, (2015).

Persian Abstract

چکیده

این مقاله به مطالعه پایداری دینامیکی سیستم چتر سرشی- محموله در طول مسیر پرواز سرش آن پرداخته است. بدین منظور و برای بررسی دقیق مشخصه‌های پاسخ دینامیکی مربوطه، پس از رهایش از ارتفاع بالا یک مدل دوجسمی بهبودیافته توسعه داده شده است. در فرآیند تحلیل پایداری، حرکت نوسانی سمتی محموله در دینامیک سیستم لحاظ گردیده است، که به نوبه خود موجب ایجاد یک ماتریس ضرایب وابسته به حالت گردیده و الگوریتم خطی سازی را مشکل می‌سازد. برای حل مسئله، یک الگوریتم مشتق‌گیری سمبلیک یکپارچه مبتنی بر ژاکوبین پیاده سازی شده و دینامیک سیستم در نقاط کاری مختلف در طول بخش سرش از مسیر طرح‌ریزی شده، خطی گردیده است. بر اساس نتایج ، سیستم چتر سرشی دقیقاً همانند هواپیما در کانال طولی دارای مودهای پریود کوتاه مدت و فیوگوید است. در کانال عرضی-سمتی، علاوه بر مود داچ رول سیستم دارای یک مود غلت و مارپیچ کوپل شده با فرکانس پایین است که منتج از زاویه آنهدرال بالای چتر است. نتایج نشان می‌دهد که در کانال عرضی-سمتی، مود کوپل شده برای زاویه های آنهدرال کوچک به دو مود متمایز غلت و مارپیچ تجزیه می‌شود. همچنین بر اساس نتایج، با نزول چتر ، دوره تناوب و نسبت میرایی برای مود پریود کوتاه ، به ترتیب ۱۸ و ۳۰ درصد افزایش می یابد. برای مود فیوگوید، دوره نوسانات ۲۰٪ کاهش یافته در حالیکه نسبت میرایی تقریباً ثابت خواهد بود. به عبارتی دیگر، با نزول چتر ، پایداری مود داچ رول کاهش می‌یابد، در حالی که مودهای دیگر پایدارتر می‌شوند. علاوه بر این، از نقطه نظر عملی، ازدیاد طول طنابهای تعلیق، پایداری مود کوپل غلت و مارپیچ را افزایش داده در حالی که پایداری مودهای دیگر کاهش خواهد یافت.